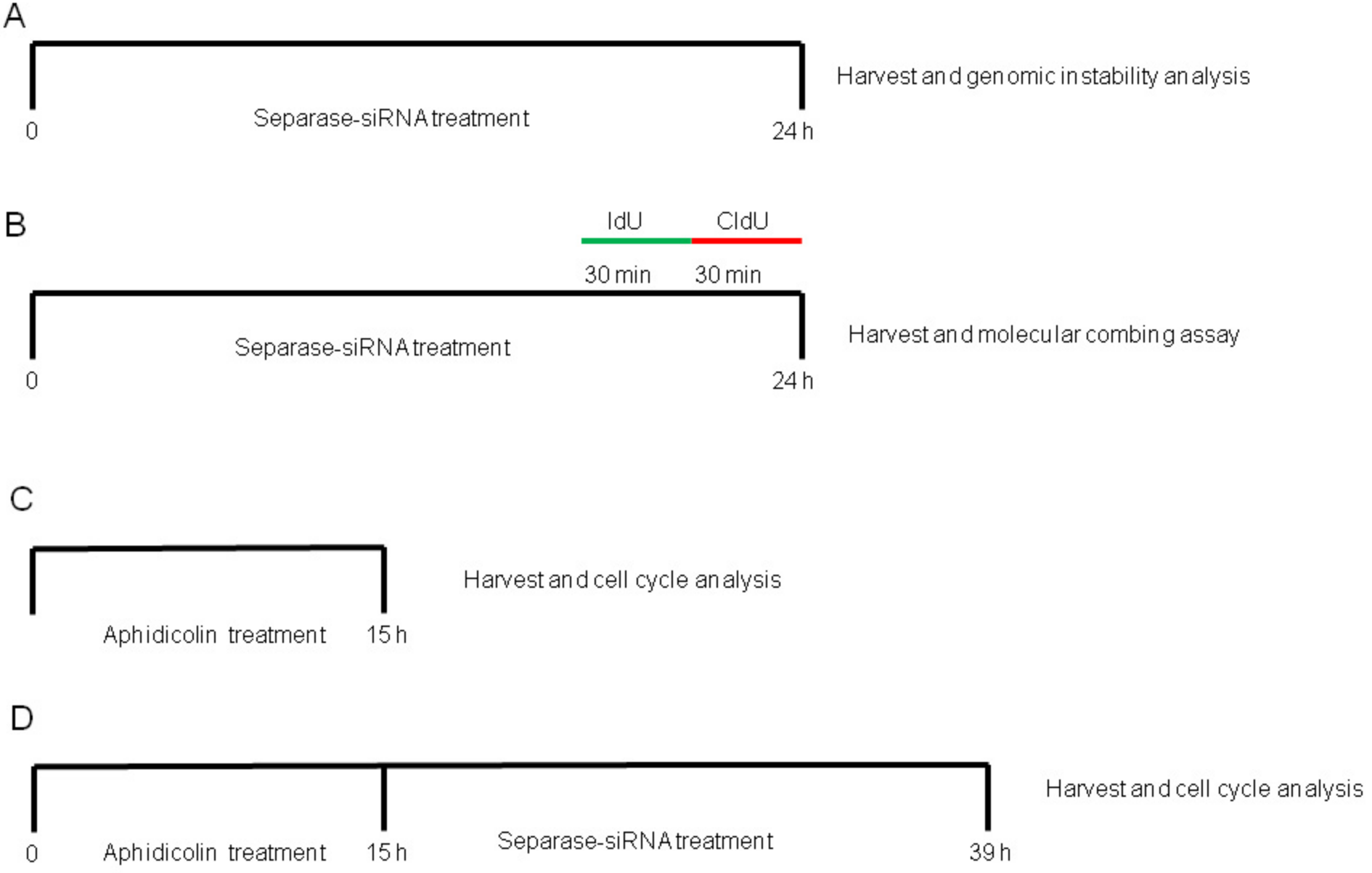
A
Harvest and genomic instability analysis
0
Separase-siRNA treatment
24 h
B
IdU
CldU
30 min
30 min
Harvest and molecular combing assay
Separase-siRNA treatment
0
24 h
C
Harvest and cell cycle analysis
Aphidicolin treatment
15 h
D
Harvest and cell cycle analysis
0
Aphidicolin treatment
15 h
Separase-siRNA treatment
39 h

Figure S1

A

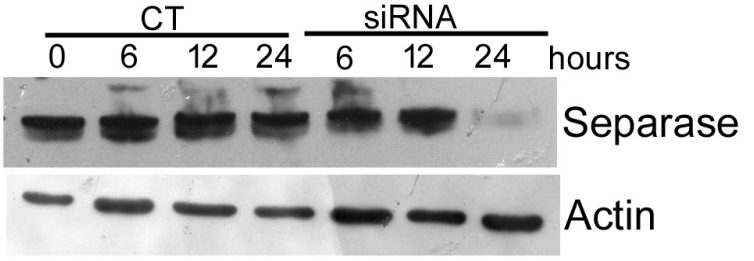
CT
siRNA
0
6
12
24
6
12
24
hours
Separase
Actin

B

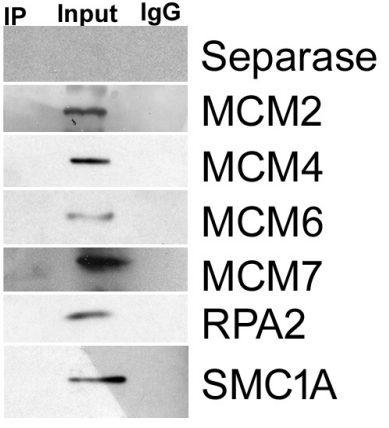
IP
Input
IgG
Separase
MCM2
MCM4
MCM6
MCM7
RPA2
SMC1A

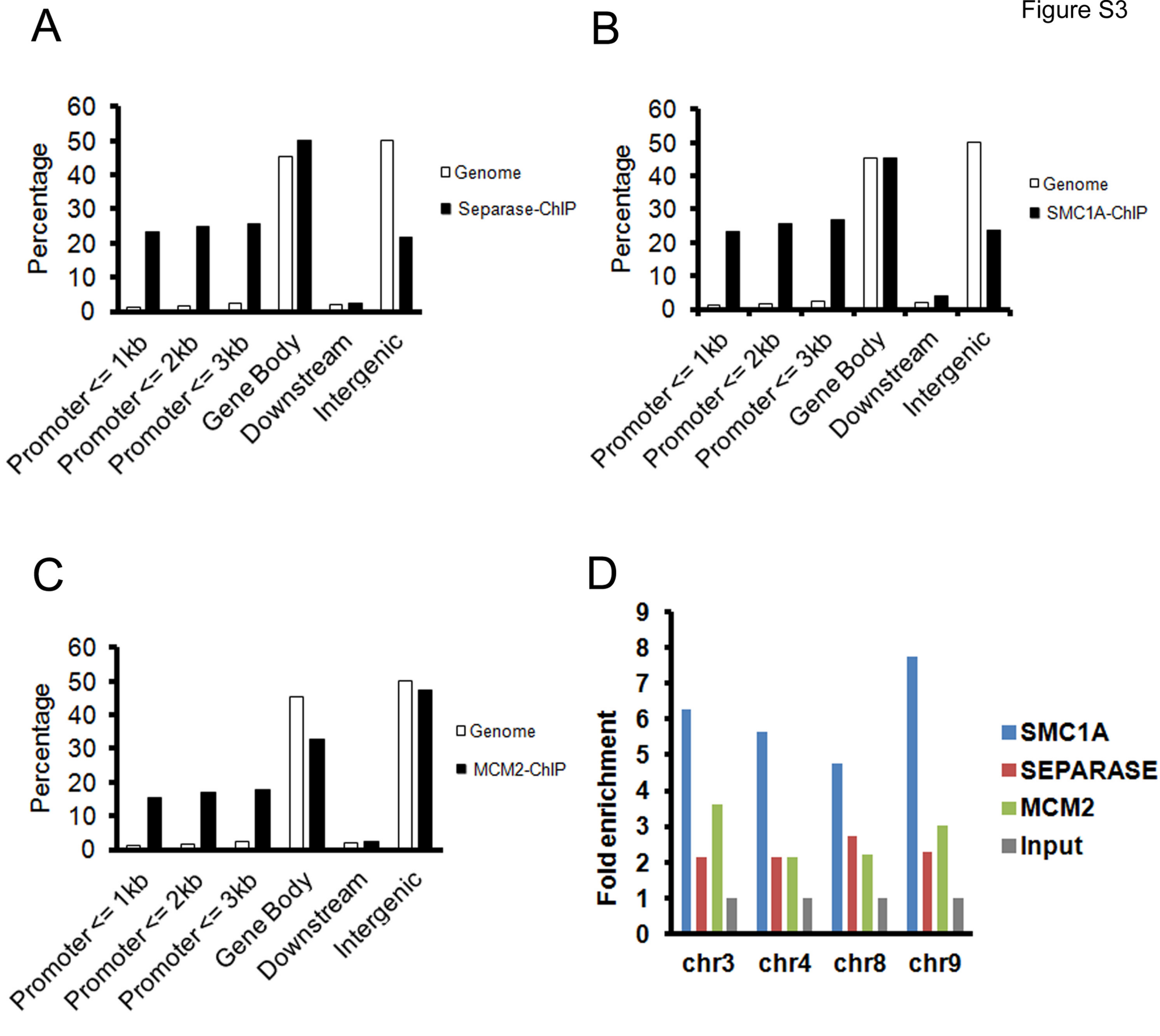
A
Percentage
60
50
40
30
20
10
0
Promoter <= 1kb
Promoter <= 2kb
Promoter <= 3kb
Gene Body
Downstream
Intergenic
Genome
Separase-ChIP
B
Percentage
60
50
40
30
20
10
0
Promoter <= 1kb
Promoter <= 2kb
Promoter <= 3kb
Gene Body
Downstream
Intergenic
Genome
SMC1A-ChIP
C
Percentage
60
50
40
30
20
10
0
Promoter <= 1kb
Promoter <= 2kb
Promoter <= 3kb
Gene Body
Downstream
Intergenic
Genome
MCM2-ChIP
D
Fold enrichment
9
8
7
6
5
4
3
2
1
0
chr3
chr4
chr8
chr9
SMC1A
SEPARASE
MCM2
Input

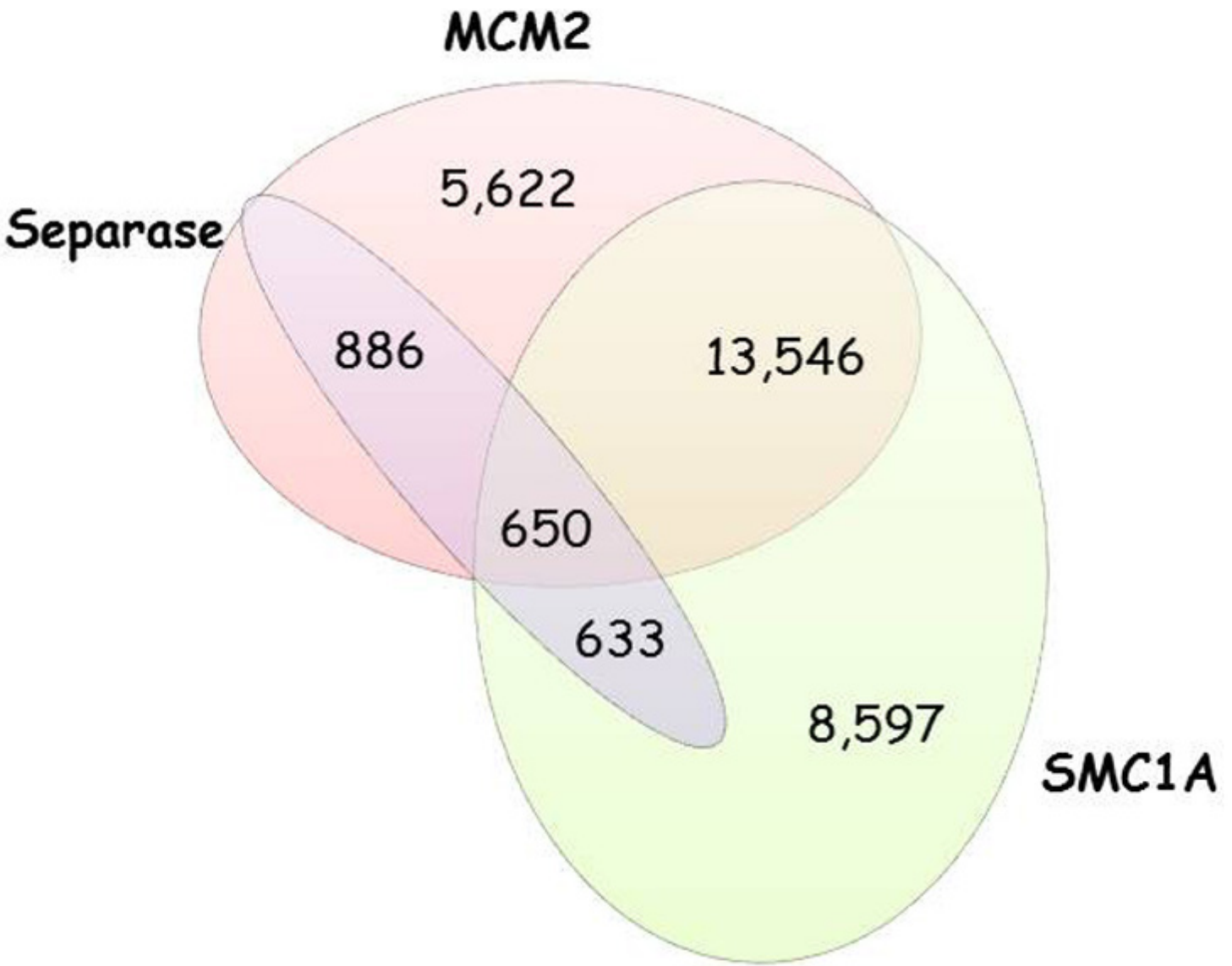
MCM2
5,622
Separase
886
13,546
650
633
8,597
SMC1A

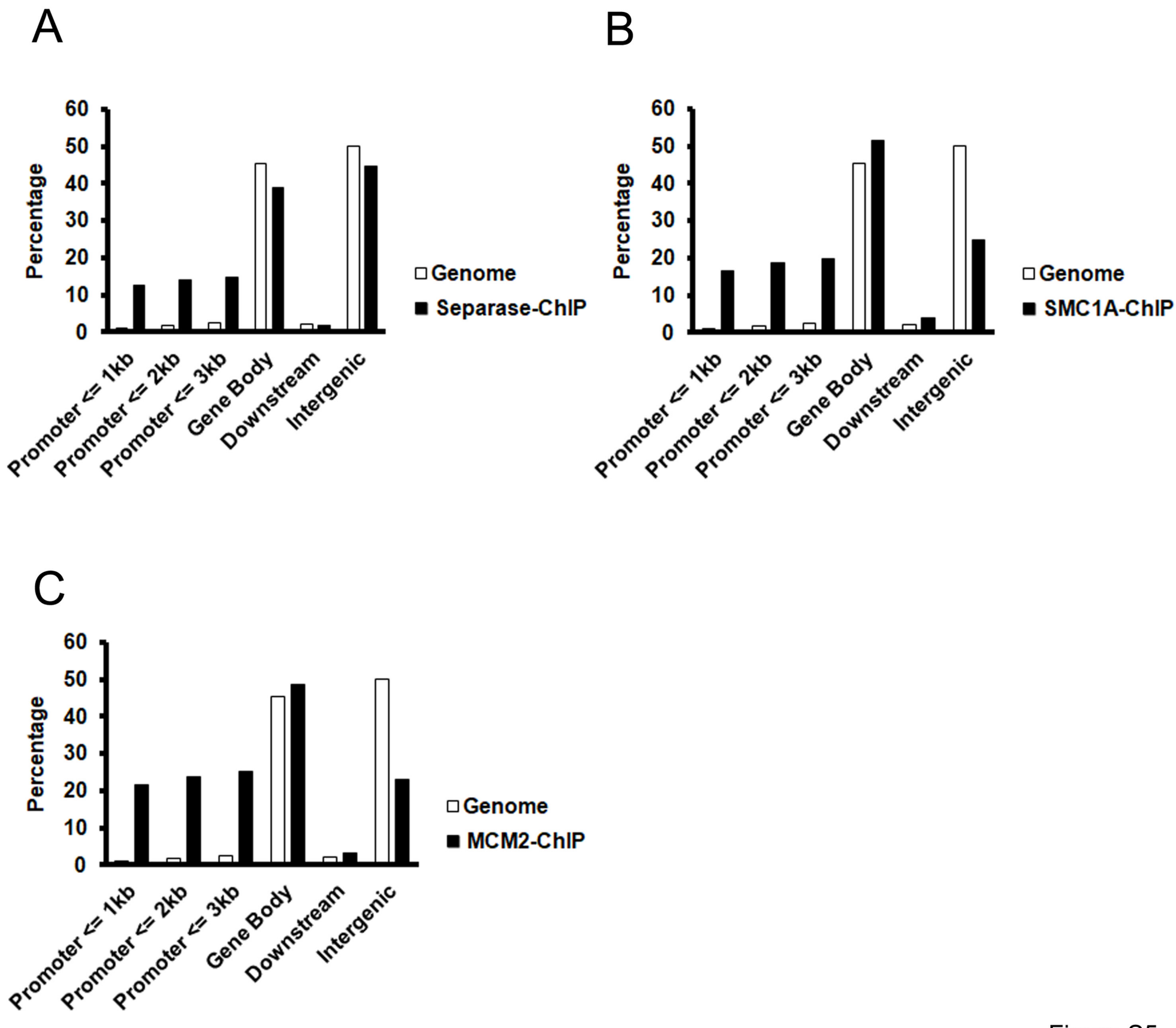
A
Percentage
60
50
40
30
20
10
0
Promoter <= 1kb
Promoter <= 2kb
Promoter <= 3kb
Gene Body
Downstream
Intergenic
Genome
Separase-ChIP
B
Percentage
60
50
40
30
20
10
0
Promoter <= 1kb
Promoter <= 2kb
Promoter <= 3kb
Gene Body
Downstream
Intergenic
Genome
SMC1A-ChIP
C
Percentage
60
50
40
30
20
10
0
Promoter <= 1kb
Promoter <= 2kb
Promoter <= 3kb
Gene Body
Downstream
Intergenic
Genome
MCM2-ChIP

Figure S5

Figure S6

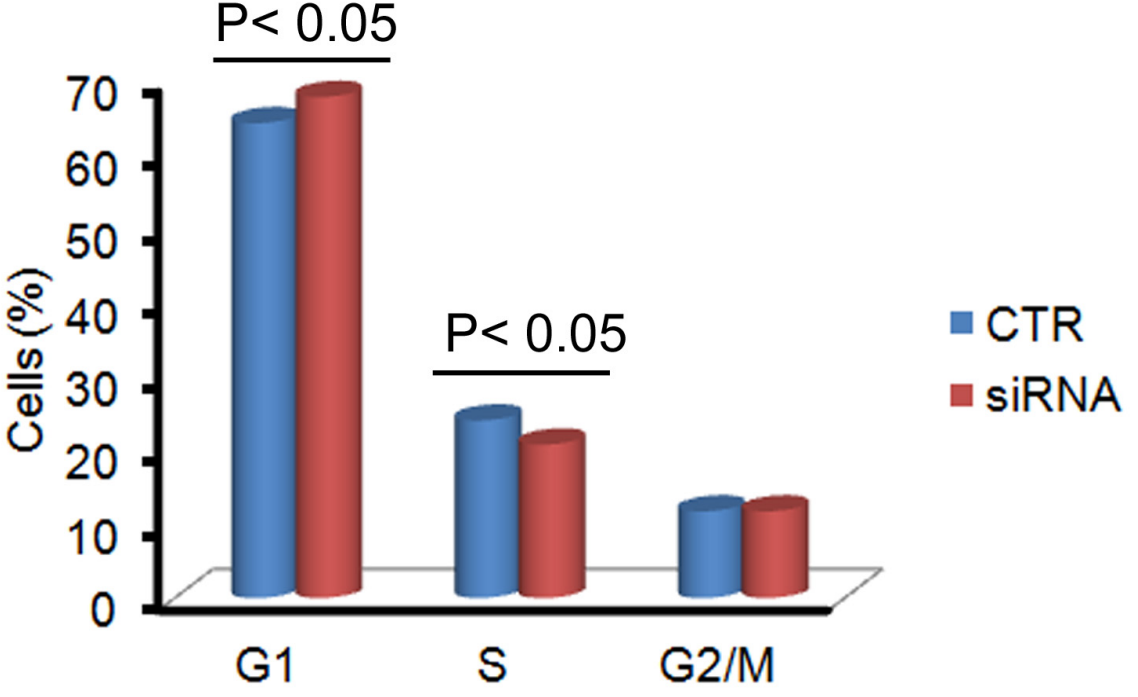

A

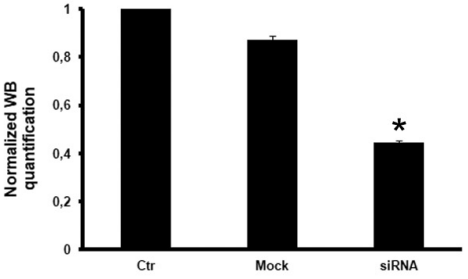
Normalized WB quantification
1
0,8
0,6
0,4
0,2
0
*
Ctr
Mock
siRNA

B

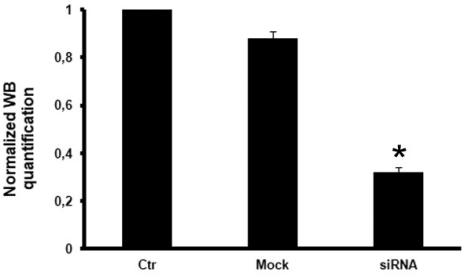
Normalized WB quantification
1
0,8
0,6
0,4
0,2
0
*
Ctr
Mock
siRNA

C

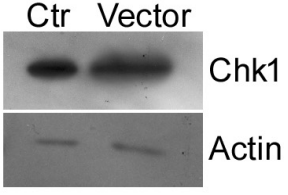
Ctr
Vector
Chk1
Actin

D

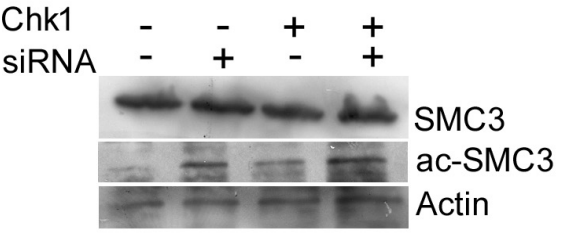
Chk1 - - + +
siRNA - + - +
SMC3
ac-SMC3
Actin

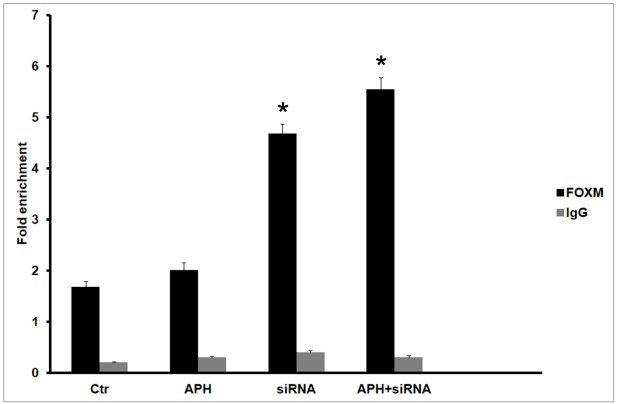
Fold enrichment
FOXM
IgG
Ctr
APH
siRNA
APH+siRNA

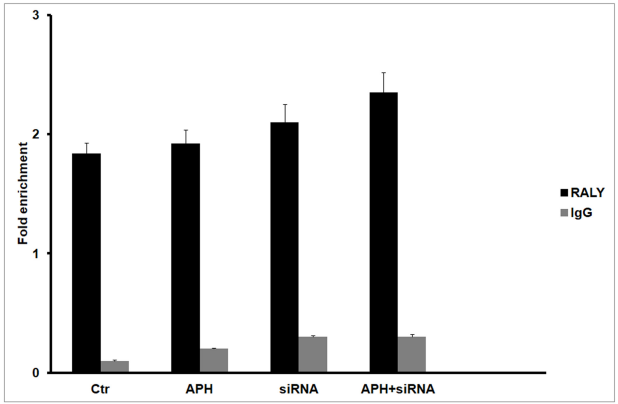
Fold enrichment
RALY
IgG
Ctr
APH
siRNA
APH+siRNA

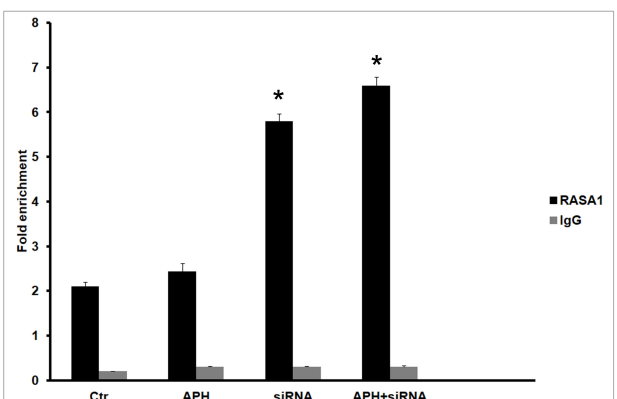
Fold enrichment
RASA1
IgG
Ctr
APH
siRNA
APH+siRNA

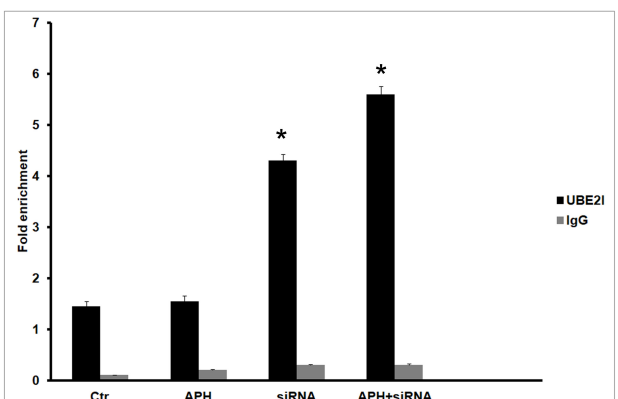
Fold enrichment
UBE2I
IgG
Ctr
APH
siRNA
APH+siRNA

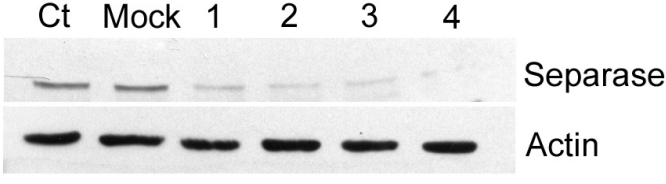
Ct
Mock
1
2
3
4
Separase
Actin

A

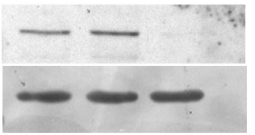
CTR Mock siRNA
Separase
Actin

B

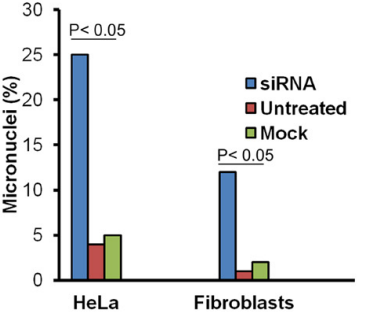
30
25
20
15
10
5
0
Micronuclei (%)
P< 0.05
P< 0.05
siRNA
Untreated
Mock
HeLa
Fibroblasts

C

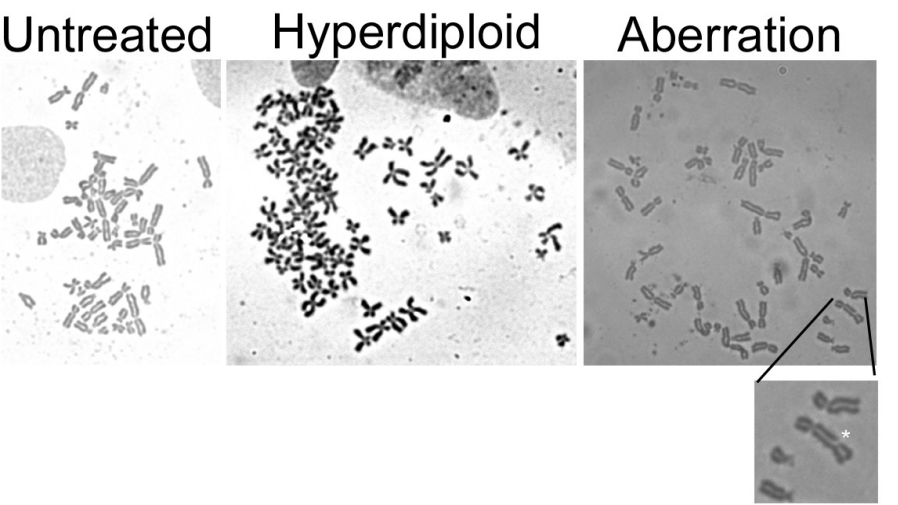
Untreated
Hyperdiploid
Aberration

Table S1. Primers used for validation of ChIP-seq data.

Chromosome	Genomic region*	Primer sequence	
3	156,544,107 to 156,544,610	F	5'- GGAACGGGGTTAGAAAGGGA - 3'
		R	5'- GGCGGGAGTTCACATCCTAA - 3'
4	141,075,155 to 141,075,714	F	5' - ACAATGATCAACTGCTCGCC - 3'
		R	5' - CGTCCTGATATCACTCCGCT - 3'
8	145,158,457 to 145,158,997	F	5' - CACAAATGGACACGGCCC - 3'
		R	5' - CCCAAAGACCAGCTCTAACG - 3'
9	140,082,977 to 140,083,419	F	5' - CGATGACGCGCTAGTTCG - 3'
		R	5' - TTGTTGTAGTTCTGCAGCGC - 3'
		R	5' - CTTTCCTGGCGTCGTTTCC - 3'

*GRCh37/hg19 genome assembly

Table S2. Primers used for ChIP-qPCR .

Gene	Forward primer sequence (5'-3')	Reverse primer sequence (5'-3')	Chromosome position
RALY	TAAAAGCGAAAGGACCAGGA	AGTGGGAGGAAGATGGAAGC	chr20:33,993,082-33,993,325
UBE2I	GCGGGAATGAGTGAGAGT	CATTCGATCCCTCCATCA	chr16:1,308,343-1,308,605
FOXM1	CCACTTCTTCCCCCACAAG	CAGTTTGTTCCGCTGTTTGA	chr12:2,877,134-2,877,322
RASA1	GAGTAGAGCGGGCTTCAACA	ACCCAGAGTTCCAGCCACT	chr5:87,268,433-87,268,637
GAPDH	AGTGTCCTGCTGCCCACAGT	TAGCCGGGCCCTACTTTCTC	chr12:6,534,207-6,534,374

Table S3. Protein identified by Mass Spectrometry analysis

Gene name	Acc Number	Protein names	Pathways
PRKDC	P78527	DNA-dependent protein kinase catalytic subunit	Cell cycle
ESPL1	Q14674	Separin	Cell cycle
SMC1A	Q14683	Structural maintenance of chromosomes protein 1A	Cell cycle
MCM4	P33991	DNA replication licensing factor MCM4	Cell cycle, DNA replication
MCM7	P33993	DNA replication licensing factor MCM7	Cell cycle, DNA replication
MCM6	Q14566	DNA replication licensing factor MCM6	Cell cycle, DNA replication
RPA2	P15927	Replication protein A 32 kDa subunit	DNA replication, Mismatch repair, Homologous recombination
RPA1	P27694	Replication protein A 70 kDa DNA-binding subunit	DNA replication, Mismatch repair, Homologous recombination
SSBP1	Q04837	Single-stranded DNA-binding protein, mitochondrial	DNA replication, Mismatch repair, Homologous recombination
DLST	P51114	Fragile X mental retardation syndrome-related protein 1	Citrate cycle (TCA cycle)
DLAT	Q14152	Eukaryotic translation initiation factor 3 subunit A	Citrate cycle (TCA cycle)
ACLY	P53396	ATP-citrate synthase	Metabolic pathways, Citrate cycle (TCA cycle)
ATP5A1	P25705	ATP synthase subunit alpha, mitochondrial	Metabolic pathways
ATP5C1	P36542	ATP synthase subunit gamma, mitochondrial	Metabolic pathways
CAD	P27708	CAD protein	Metabolic pathways
PFAS	O15067	Phosphoribosylformylglycinamidine synthase	Metabolic pathways
QARS	P47897	Glutamine--tRNA ligase	Metabolic pathways
PTDSS1	P48651	Phosphatidylserine synthase 1	Metabolic pathways
FASN	P49327	Fatty acid synthase	Metabolic pathways
SMS	P52788	Spermine synthase	Metabolic pathways, Arginine and proline metabolism
ALDH18A1	P54886	Delta-1-pyrroline-5-carboxylate synthase	Metabolic pathways, Biosynthesis of amino acids, Arginine and proline metabolism
ARG1	P05089	Arginase-1	Metabolic pathways, Biosynthesis of amino acids, Arginine and proline metabolism
PRPS2	P11908	Ribose-phosphate pyrophosphokinase 2	Metabolic pathways, Biosynthesis of amino acids, Arginine and proline metabolism, Carbon metabolism, Pentose phosphate pathway
DLST	P36957	Dihydrolipoyllysine-residue succinyltransferase component of 2-oxoglutarate dehydrogenase complex	Metabolic pathways, Carbon metabolism
PC	P11498	Pyruvate carboxylase, mitochondrial	Metabolic pathways, Carbon metabolism, Citrate cycle (TCA cycle), Biosynthesis of amino acids
PGK1	P00558	Phosphoglycerate kinase 1	Metabolic pathways, Carbon metabolism, Glycolysis / Gluconeogenesis, Biosynthesis of amino acids
PKM	P14618	Pyruvate kinase PKM	Metabolic pathways, Carbon metabolism, Glycolysis / Gluconeogenesis, Biosynthesis of amino acids
PFKL	P17858	ATP-dependent 6-phosphofructokinase, liver type	Metabolic pathways, Carbon metabolism, Glycolysis / Gluconeogenesis, Pentose phosphate pathway, Biosynthesis of amino acids

DLAT	P10515	Dihydrolipoyllysine-residue acetyltransferase component of pyruvate dehydrogenase complex	Metabolic pathways, Glycolysis / Gluconeogenesis, Carbon metabolism
GANAB	Q14697	Neutral alpha-glucosidase AB	Metabolic pathways, Protein processing in endoplasmic reticulum
CPS1	P31327	Carbamoyl-phosphate synthase	Metabolic pathways,Carbon metabolism, Biosynthesis of amino acids, Arginine and proline metabolism
HSP90AA1	P07900	Heat shock protein HSP 90-alpha	Protein processing in endoplasmic reticulum
HSP90AB1	P08238	Heat shock protein HSP 90-beta	Protein processing in endoplasmic reticulum
EIF2AK2	P19525	Interferon-induced, double-stranded RNA-activated protein kinase	Protein processing in endoplasmic reticulum
DNAJA1	P31689	DnaJ homolog subfamily A member 1	Protein processing in endoplasmic reticulum
SSR1	P43307	Translocon-associated protein subunit alpha	Protein processing in endoplasmic reticulum
CKAP4	Q07065	Cytoskeleton-associated protein 4	Protein processing in endoplasmic reticulum
RPLP0	P05388	60S acidic ribosomal protein P0	Ribosome
RPS2	P15880	40S ribosomal protein S2	Ribosome
RPL17	P18621	60S ribosomal protein L17	Ribosome
RPL10	P27635	60S ribosomal protein L10	Ribosome
RPL9	P32969	60S ribosomal protein L9	Ribosome
RPL22	P35268	60S ribosomal protein L22	Ribosome
RPL4	P36578	60S ribosomal protein L4	Ribosome
RPS19	P39019	40S ribosomal protein S19	Ribosome
RPL3	P39023	60S ribosomal protein L3	Ribosome
RPL15	P61313	60S ribosomal protein L15	Ribosome
RPS8	P62241	40S ribosomal protein S8	Ribosome
RPS15A	P62244	40S ribosomal protein S15a	Ribosome
RPS16	P62249	40S ribosomal protein S16	Ribosome
RPS14	P62263	40S ribosomal protein S14	Ribosome
RPS23	P62266	40S ribosomal protein S23	Ribosome
RPS11	P62280	40S ribosomal protein S11	Ribosome
RPL7A	P62424	60S ribosomal protein L7a	Ribosome
RPS6	P62753	40S ribosomal protein S6	Ribosome
RPL23	P62829	60S ribosomal protein L23	Ribosome
RPS26	P62854	40S ribosomal protein S26	Ribosome
RPL10A	P62906	60S ribosomal protein L10a	Ribosome
RPL11	P62913	60S ribosomal protein L11	Ribosome
RPL18A	Q02543	60S ribosomal protein L18a	Ribosome
RPL36	Q9Y3U8	60S ribosomal protein L36	Ribosome
XPO1	O14980	Exportin-1	RNA transport
NUP155	O75694	Nuclear pore complex protein Nup155	RNA transport
TPR	P12270	Nucleoprotein TPR	RNA transport
FXR1	P51114	Fragile X mental retardation syndrome-related protein 1	RNA transport
NUP160	Q12769	Nuclear pore complex protein Nup160	RNA transport
EIF3A	Q14152	Eukaryotic translation initiation factor 3 subunit A	RNA transport
NUP210	Q8TEM1	Nuclear pore membrane glycoprotein 210	RNA transport
PRPF40A	O75400	Pre-mRNA-processing factor 40 homolog A	Spliceosome
SRSF10	O75494	Serine/arginine-rich splicing factor 10	Spliceosome
SNRNP200	O75643	U5 small nuclear ribonucleoprotein 200 kDa helicase	Spliceosome
DDX5	P17844	Probable ATP-dependent RNA helicase DDX5	Spliceosome

U2AF2	P26368	Splicing factor U2AF 65 kDa subunit	Spliceosome
HNRNPA3	P51991	Heterogeneous nuclear ribonucleoprotein A3	Spliceosome
HNRNPM	P52272	Heterogeneous nuclear ribonucleoprotein M	Spliceosome
HNRNPK	P61978	Heterogeneous nuclear ribonucleoprotein K	Spliceosome
TRA2B	P62995	Transformer-2 protein homolog beta	Spliceosome
SRSF1	Q07955	Serine/arginine-rich splicing factor 1	Spliceosome
SF3A1	Q15459	Splicing factor 3A subunit 1	Spliceosome
PRPF8	Q6P2Q9	Pre-mRNA-processing-splicing factor 8	Spliceosome

Table S4. Replication parameters in control and *Separase*-silenced HeLa cells.

	CTR	siRNA
Fork rate (kb/min)**		
Median	0.57	0.90
Average	0.59	0.92
SD	0.280	0.280
SE	0.037	0.035
N	58	64
Inter-origin distance (kb)**		
Median	65.2	98.7
Average	84.9	130.1
SD	60.38	100.64
SE	6.10	9.26
N	98	118
Cluster length (kb)		
Median	494.4	649.7
Average	578.0	753.6
SD	377.10	439.48
SE	58.19	63.43
N	42	48
Origin number/cluster		
Median	6	5
Average	6	5
SD	3.6	2.4
SE	0.6	0.3
N	42	48
DNA molecule length (kb)		
Median	751.5	934.8
Average	910.4	1061.8
SD	436.17	463.41
SE	67.30	66.89
N	42	48
Unidirectional forks*		
Unidirectional/total	86/174	60/158
%	49.4	38.0
Paused/arrested forks		
Paused/arrested/total	25/174	24/158
%	14.4	15.2
Asynchronous forks		
Asynchronous/total	5/174	10/158
%	2.9	6.3

SD: standard deviation; SE: standard error.
**: P< 0.001
*: P< 0.05

Supplementary Figure Legends

Figure S1. Flow chart describing experimental protocols used in this work. (**A**) Cells were treated with siRNA against *Separase* for 24 hours and immediately analyzed for genomic instability. (**B**) HeLa cells were treated with Separase-siRNA for 24 hour; during the last hour cells were labelled with IdU for 30 min, washed and then pulsed with CldU for a further 30 min. Thereafter, cells were harvested and assayed with molecular combing technique. (**C**) Cells were treated with aphidicolin for 15 hours. (**D**) In order to investigate the effect of *Separase* depletion on stalled forks, first the cells were treated with aphidicolin for 15 hours and then separase was depleted by siRNA treatment for the following 24 hours. Time length is not in scale.

Figure S2. Effect of *Separase* silencing. **(A)** Time course (6, 12 and 24 hours) analysis of siRNA treatment. **(B)** *Separase* depletion affects the interaction with replisome proteins.

Figure S3. Genome-wide distribution of Separase, SMC1A and MCM2 binding sites. (**A**) Separase. (**B**) SMC1A. (**C**) MCM2 binding sites in HeLa cells represented as percentage of sites detected at promoter, downstream, gene body and intergenic regions. Peaks were aligned to RefSeq gene annotations by the use of CEAS tool. We compared binding of Separase, SMC1A and MCM2 to a selected region to the average genome-wide binding. (**D**) ChIP-seq data were validated by qPCR. Fold enrichment of MCM2, Separase and SMC1A was calculated relative to Input in four genomic regions on chromosomes 3, 4, 8 and 9 in which MCM2, Separase and SMC1A co-localize.

Figure S4. Separase co-localizes with SMC1A and MCM2. Venn diagram showing the overlap between Separase, MCM2 and SMC1A as determined by ChIP-seq in cells synchronized in S-phase by aphidicolin treatment for 15 hours.

Figure S5. Genome-wide distribution of Separase, SMC1A and MCM2 binding sites following cell synchronization in S-phase by aphidicolin. (**A**) Separase. (**B**) SMC1A. (**C**) MCM2 binding sites in HeLa cells represented as percentage of sites detected at promoter, downstream, gene body and intergenic regions. Peaks were aligned to RefSeq gene annotations by the use of CEAS tool. We compared binding of Separase, SMC1A and MCM2 to a selected region to the average genome-wide binding.

Figure S6. *Separase* silencing reduces the frequency of cells in S-phase. HeLa cells were treated with siRNA against *Separase* for 24 hours and DNA content was analyzed by flow cytometry. The values are the mean of three independent experiments.

Figure S7. Effects of Chk1 overexpression in HeLa cells. (**A**) Quantification of Chk1level with respect to Actin from three different blottings after *Separase* depletion. (**B**) Quantification of pS345-Chk1following *Separase* ablation. (**C**) Western blot analysis of extracts from untreated (Ctr) and treated with a vector overexpressing Chk1. (**D**) Effects of Chk1 overexpression and *Separase*-siRNA treatments on SMC3 and acetylated-SMC3 levels. *$p < 0.05$.

Figure S8. Analysis of SMC1A occupancy at the promoter regions. Cohesin binding in *FOXM, RALY, RASA1* and *UBE2I* genes in unsynchronized and synchronized cells. IgG was used as negative control. Results represent three independent ChIP assays and the average values of the experiments and the relative standard errors are shown.* $p < 0.05$.

Figure S9. siRNA treatments against *Separase*. HeLa cells were treated with four different siRNAs against *Separase*. Target sequences are reported in Material and Methods.

Figure S10. Effects of *Separase* depletion on genome stability. (**A**) Primary fibroblast cells were transfected with siRNA against *Separase*. Twenty-four hours after transfection, total cell lysates were analyzed by immunoblotting with Separase and Actin (as loading control) antibodies. (**B**) The frequency of micronuclei which arise as a consequence of missegregation was higher ($P < 0.05$) in treated cells when compared in control cells. (**C**) Karyotypic analysis of 100 Giemsa staining metaphase spreads revealed the presence of hyperdiploid cells and structural chromosome aberrations. A chromosome break is highlighted.